






Optimal Grid Layouts for Hybrid Offshore Assets in the North Sea under Different Market Designs

Stephen Hardy¹ , Andreas Themelis² , Kaoru Yamamoto² *Member, IEEE*, , Hakan Ergun¹ *Senior Member, IEEE*,  and Dirk Van Hertem¹ *Senior Member, IEEE*, 

¹KU Leuven/EnergyVille, Leuven/Genk, Belgium ²Kyushu University, Fukuoka, Japan

Abstract—This work examines the Generation and Transmission Expansion (GATE) planning problem of offshore grids under different market clearing mechanisms: a Home Market Design (HMD), a zonal cleared Offshore Bidding Zone (zOBZ) and a nodal cleared Offshore Bidding Zone (nOBZ). It aims at answering two questions.

- 1) Is knowing the market structure a priori necessary for effective generation and transmission expansion planning?
- 2) Which market mechanism results in the highest overall social welfare?

To this end a multi-period, stochastic GATE planning formulation is developed for both nodal and zonal market designs. The approach considers the costs and benefits among stake-holders of Hybrid Offshore Assets (HOA) as well as gross consumer surplus (GCS). The methodology is demonstrated on a North Sea test grid based on projects from the European Network of Transmission System Operators' (ENTSO-E) Ten Year Network Development Plan (TYNDP). An upper bound on potential social welfare in zonal market designs is calculated and it is concluded that from a generation and transmission perspective, planning under the assumption of an nOBZ results in the best risk adjusted return.

Index Terms—Expansion planning, grid topology, meshed HVDC grids, mixed-integer optimization, offshore wind energy, power generation, power transmission.

NOMENCLATURE

\mathcal{A}^{br}	Balancing responsible optimization variables
\mathcal{A}^{te}	Transmission expansion optimization variables
\mathcal{A}_j	Storage developer optimization variables
\mathcal{A}_o	Transmission developer optimization variables
\mathcal{A}_w	OWPP developer optimization variables
$\alpha^{\ell, \text{br}}$	Intra-zonal candidate line binary decision variable
$\alpha^{\ell, \text{te}}$	Inter-zonal candidate line binary decision variable
α^{ℓ}	Candidate line binary decision variable
$\mathcal{P}^{\text{j,abs}}$	Set of storage absorption power variables.
$\mathcal{P}^{\text{j,inj}}$	Set of storage injection power variables.
\mathcal{P}^{u}	Set of instantaneous demand variables.
α^{ℓ}	Set of candidate transmission line variables.
θ	Set of voltage angle variables.
$\tilde{\mathcal{P}}^{\text{g}}$	Set of candidate generator output variables.
$\bar{\mathcal{P}}^{\text{g}}$	Set of existing generator output variables.

$\tilde{\mathcal{S}}_{\text{g}}$	Set of candidate generators
$\tilde{\mathcal{S}}_{\ell}$	Set of candidate transmission lines
θ	Candidate voltage angle
$\Delta\theta^{\text{max}}$	Maximum voltage angle difference
$\Delta E^{\text{j,max}}$	Change in storage capacity
δI^{ζ}	Converter expansion investment
δI^{g}	Generation expansion investment
δI^{j}	Storage expansion investment
$\Delta \mathcal{P}^{\text{g,max}}$	Change in generation capacity
$\Delta \mathcal{P}^{\zeta, \text{max}}$	Change in converter capacity
$\Delta E^{\text{j,max}}$	Set of change in max storage capacity variables.
$\Delta \mathcal{P}^{\zeta, \text{max}}$	Set of change in max converter capacity variables.
$\Delta \tilde{\mathcal{P}}^{\text{g,max}}$	Set of change in max generator capacity variables.
\mathcal{E}	Set of all (directed) edges
\mathcal{E}^{AC}	Set of AC network edges
\mathcal{E}^{DC}	Set of DC network edges
\mathcal{E}^{br}	Set of intra-zonal edges
\mathcal{E}^{te}	Set of inter-zonal edges
$\mathcal{E}^{\text{AC-DC}}$	Set of all edges between AC and DC networks
$\eta^{\text{j,abs}}$	Charge efficiency of storage
$\eta^{\text{j,inj}}$	Discharge efficiency of storage
$\tilde{\mathcal{S}}_{\text{g}}$	Set of existing generators
$\tilde{\mathcal{S}}_{\ell}$	Set of existing transmission lines
γ^{j}	Self-discharge rate
λ	Market clearing price
\mathcal{N}	Set of all nodes
\mathcal{N}^{AC}	Set of all AC nodes
\mathcal{N}^{DC}	Set of all DC nodes
π_s	Probability of scenario s
Ψ^{g}	RES generator time series
Ψ^{u}	Demand time series
\mathcal{S}_{g}	Set of all generators
\mathcal{S}_{j}	Set of storage devices
\mathcal{S}_{ℓ}	Set of all transmission lines
\mathcal{S}_{s}	Set of scenarios
\mathcal{S}_{t}	Set of hours
\mathcal{S}_{u}	Set of demands
\mathcal{S}_{y}	Set of years
τ	Transformer ratio
θ	Voltage angle
θ^{max}	Maximum voltage angle
θ^{min}	Minimum voltage angle
$\widehat{E^{\text{j,max}}}$	Maximum expansion capacity of candidate storage
$\widehat{P^{\text{g,max}}}$	Maximum expansion capacity of candidate generators
$\widehat{P^{\zeta, \text{max}}}$	Maximum expansion capacity of candidate converters

This project has received funding from the CORDOBA project funded by Flanders Innovation and Entrepreneurship (VLAIO) in the framework of the spearhead cluster for blue growth in Flanders (Blue Cluster) – Grant number HBC.2020.2722, and from the Japan Society for the Promotion of Science (JSPS) KAKENHI grants no. JP19H02161, JP20K14766 and JP21K17710. A special thanks to Michiel Kenis and Prof. Jef Berten for their input regarding energy market modelling.

$\xi^{j,c}$	Maximum charge rate
$\xi^{j,d}$	Maximum discharge rate
\mathcal{Z}	Set of market zones
b	Transmission line susceptance
C^g	Generator bid price
C^u	Consumer bid price
$E^{j,\max}$	Maximum capacity of candidate storage
E^j	Capacity of candidate storage
f^H	NPV scalar for hourly revenues
f^Y	NPV scalar for yearly revenues
I^ℓ	Candidate line investment
L^ζ	Converter loss factor
$P^{\ell,\max}$	Maximum transmission line power
P^ℓ	Instantaneous Transmission line power
$P^{g,\max}$	Maximum generator power
P^g	Instantaneous generator power
$P^{j,\text{abs}}$	Instantaneous storage charging power
$P^{j,\text{inj}}$	Instantaneous storage discharging power
$P^{u,\max}$	Maximum demand power
P^u	Instantaneous demand power
$P^{\zeta,\max}$	Maximum converter power
$P^{\zeta,\text{AC}}$	Instantaneous AC side converter power
$P^{\zeta,\text{DC}}$	Instantaneous DC side converter power
$P^{\zeta,\text{loss}}$	Instantaneous converter power losses
T	Hours per simulation year

I. INTRODUCTION

A. Motivation

A perfect storm has descended on the European energy landscape. The ever pressing issues of climate change have converged with an urgent need to reduce the dependence on Russian gas in light of the recent invasion of Ukraine. In response to the invasion, the European Commission recently presented the 300 B€ REpowerEU plan to rapidly scale-up Renewable Energy Sources (RESs) and network electrification. The plan builds on the already ambitious targets under the Fit for 55 plan, increasing renewable generation targets to 1236 GW from 1067 GW by 2030 [1].

Offshore wind in the North Sea is crucial in meeting these targets. The North Sea governments of Belgium, Denmark, the Netherlands and Germany have pledged to increase the installed capacity of North Sea offshore wind farms to 65 GW by 2030 and to 150 GW by 2050 [2]. This is a substantial step towards the EU wide goal of 240 to 450 GW of offshore wind by 2050, which is needed to meet the climate targets agreed upon under The Paris Agreement [3], [4].

In addition to expanding offshore wind, investments in transmission infrastructure are required. To this end, the European Network of Transmission System Operators for Electricity (ENTSO-E) releases a Ten Year Network Development Plan (TYNDP) every two years to identify essential infrastructure investments [5]. To date, 43 offshore transmission projects, including interconnectors, Hybrid Offshore Assets (HOAs) and Offshore Wind Power Plant (OWPP) connections, totalling 65.6 GW of capacity, are set to be commissioned by 2035. The number of projects is set to increase further as according to EU regulation 2022/869, article 14, by 2024 the

TYNDP must include a high level infrastructure investment plan for each of the sea-basins under development [6].

B. Background

Long term planning: Much research into regulatory, technological and economic aspects of a North Sea grid has been performed [7]–[9]. There is a consensus that such a grid would be a meshed High Voltage Direct Current (HVDC) grid. The economic and technical advantages of choosing HVDC are summarized in [10] while some of the technical challenges can be found in [11].

The Generation and Transmission Expansion (GATE) planning problem aims at determining the least cost power system design and in its complete form is an Mixed Integer Non-Linear Program (MINLP) [12]. Due to the difficulty of solving such a problem, the reactive power component of the non-linear power flow equations is often ignored and a linear “DC” power flow [13] or convex relaxation such as [14]–[16] assumed.

In its most common form the problem takes a central planner’s perspective as in [17], [18]. Another common way to formulate it is as an equilibrium model such as [19], [20]. The problem can be formulated as static (single time step) [19], [21] or dynamic (multi-step) problem [22], [23]. Uncertainty is often handled using stochastic programming as in [24]–[26] or robust optimization as in [27]–[29]. When analyzing energy markets with zonal market clearing, multi-level programming such as in [30], [31] has been used.

Energy Markets: In liberalized energy markets both nodal and zonal market structures can be found. Examples of the former can be found in North America while in Europe a zonal based system is the norm. For further details on market design, we refer the readers to [32], [33].

A topic currently under debate is the structure of the energy market for an offshore grid and in particular HOAs [32]. HOAs yield benefits for both OWPPs and grid expansion in unison, combining transmission, generation and storage into a single asset. For individual stakeholders, however, there is high uncertainty in expected profitability based on market design and regulation. Currently, there are three market designs under serious consideration, the Home Market Design (HMD), the zonal Offshore Bidding Zone (zOBZ) and the nodal Offshore Bidding Zone (nOBZ) [34]. In an HMD, HOAs are considered part of the energy market of the Exclusive Economic Zone (EEZ) within which they are situated. In a zOBZ, multiple or all HOAs are grouped into a common offshore market zone with a single market price. In an nOBZ all HOAs are in independent market zones, permitting fully localized energy pricing based on inter-nodal congestion.

Contributions and paper structure: In this work an agent based, multi-level, multi-period, stochastic, Mixed Integer Linear Program (MILP) is developed. The model builds on the one presented in [35] and leverages the PowerModels(ACDC).jl packages in the Julia programming language to implement the power flow equations [15], [36], [37]. The Gurobi solver version 0.9.14 [38] is used for the MILP.

The main contributions of this work are:

- A modelling formulation for different market structures within the GATE planning problem.
- A measurement of the upper bound on social welfare when considering a zonal market design.
- A cost-benefit analysis of a North Sea test case comparing an HMD, an nOBZ and a zOBZ.

The structure of the paper is as follows. In the next section a brief discussion on nodal and zonal markets is presented. Following this, the modelling methodology is described. This begins with the nodal market model in §III-A and is followed in §III-B by the zonal market model. In §IV the North Sea test grid is described along with the modelling assumptions. In §V the results are presented. Finally, in §VI, conclusions and recommendations based on the modelling results round out the paper.

II. NODAL VERSUS ZONAL MARKETS

In the interest of transparency, the authors of this study declare a pre-existing bias towards nodal pricing due to the price signals in regards to network inefficiencies such as congestion and under supply. These signals can be suppressed in a zonal system and are of very high value, especially at a time of such anticipated network expansion. It is opinioned that localized pricing should be the default and any deviation should be done with caution and only when supported by strong evidence.

Despite the known benefits of nodal pricing, it is possible to find examples where zonal pricing results in an arguably better outcome for consumers. In studying such examples we hope to meaningfully contribute to the ongoing debate regarding North Sea market structure. To illustrate this point we present a simplified market clearing example involving a pivotal supplier. The assumed market structure is a day-ahead pay-as-cleared (uniform pricing method) market [39] with imbalances settled via an idealized Regulatory re-Dispatch with Cost Compensation (RDCC) [40]. Market participants are assumed to bid truthfully at their marginal price of production.

In the pivotal supplier scenario, we have a topology similar to that of fig. 1. At node m , 5 MW of wind generation is present. At node n , 5 MW of PV, 5 MW of thermal generation and 10 MW of demand are present. A transmission line with a maximum capacity of 4 MW connects nodes m and n . Assumed marginal generation costs for RESs and thermal generation are 10 €/MWh and 100 €/MWh respectively.

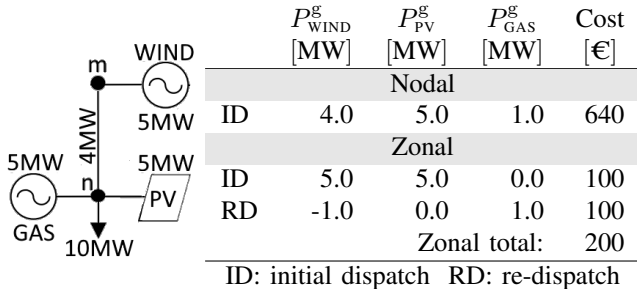


Figure 1: Single line diagram of simple market clearing topology (left). Dispatch and re-dispatch amounts and costs in nodal and zonal market clearing mechanisms (right).

In the nodal market clearing model the 4 MW capacity limit between node m and n is considered from the start, resulting in an optimal dispatch of 4 MW of wind at node m , 5 MW of PV at node n and 1 MW of thermal at node n . The resulting clearing prices are 10 €/MWh at node m and 100 €/MWh at node n . The total cost of supplying the load is 640 €.

Contrasting this with the zonal clearing model, the line congestion between m and n is initially ignored resulting in an optimal dispatch of 5 MW of wind at node m and 5 MW of PV at node n with a zonal clearing price of 10 €/MWh. The cost prior to re-dispatch is therefore 100 €. As the capacity constraint from node m to n is violated, however, the balancing authority directs the down regulation of wind to 4 MW at node m and up regulation of the thermal plant at node n to 1 MW. The balancing responsible pays a total re-dispatch cost of 100 € to the thermal plant and the total cost to supply the load is 200 € (assuming no avoided variable costs for the OWPP).

This is arguably a more desirable result for consumers. Of course, in the case of the pivotal supplier it can be correctly argued that the efficiency of the market is creating a high clearing price to signal that either additional transmission from m to n or additional generation at node n is needed. However, in a grid with high penetration of highly fluctuating sources, it may be an unusually low wind or solar irradiation day that transforms a certain generator into a pivotal supplier. The question as to whether an investment to increase transmission or generation is warranted is more complicated, as it depends on the frequency with which the pivotal supplier negatively impacts energy prices.

III. PLANNING MODEL

Special notation:

- $x : n$ (x located at node n).
- $x : mn$ (x located on directed edge mn).
- $x : \{mn\}$ (x located on undirected edge mn).

A. Nodal Market Model

1) *Objective Function:* An existing network operator (\mathcal{A}_e) and a set of developers of OWPPs (\mathcal{A}_w), offshore transmission (\mathcal{A}_o) and storage (\mathcal{A}_s) have costs and benefits associated with their operation and development as defined in (1) to (4). The costs and benefits are divided into two distinct parts: hourly operational costs and benefits and yearly strategic investments. The Net Present Value (NPV) equivalents of hourly and yearly revenue and expenditure streams are determined by scalars f_y^H and f_y^Y respectively. A discount rate of 4% is assumed.

An OWPP developer (\mathcal{A}_w) can make a strategic yearly investment to expand the capacity of an OWPP ($\Delta P_{\tilde{g}}^{max}$) as in (1a). Hourly benefits can then be accrued by selling the energy generated on the spot market at a price λ_n . The marginal cost of production is assumed to be zero.

$$U_{y,s}^w = -f_y^Y [(1a)] \quad (1)$$

$$\sum_{n \in \mathcal{N}^{ac}} \sum_{\tilde{g} \in \tilde{\mathcal{S}}_{g;n}} \delta I_{\tilde{g};n,y}^g \cdot \Delta P_{\tilde{g};n,y}^{g,max} \quad (1a)$$

An offshore transmission developer (\mathcal{A}_o) can make a strategic yearly investment to build new transmission lines (α_t^ℓ) as in (2a) and/or expand HVDC converter capacity ($\Delta P_{ne}^{\zeta, \max}$) as in (2b). Hourly benefits are then accrued through spatial arbitrage of price differentials ($\lambda_m - \lambda_n$) located in different energy markets. This is also known as congestion rent.

$$\mathcal{U}_{y,s}^o = -f_y^Y \left[(2a) + (2b) \right] \quad (2)$$

$$\sum_{\substack{\{mn\} \subseteq \mathcal{N} \\ mn \in \mathcal{E}}} \sum_{\tilde{l} \in \tilde{\mathcal{S}}_{\ell: \{mn\}}} \alpha_{t: \{mn\}, y}^\ell \cdot I_{t: \{mn\}, y}^\ell \quad (2a)$$

$$\sum_{n \in \mathcal{E}^{\text{AC-DC}}} \delta I_{ne, y}^\zeta \cdot \Delta P_{ne, y}^{\zeta, \max} \quad (2b)$$

A storage developer (\mathcal{A}_j) can make a strategic yearly investment to expand storage capacity ($\Delta E_j^{j, \max}$) as in (3a). Hourly benefits are then accrued through temporal arbitrage of price differentials ($\lambda_{n,t} - \lambda_{n,t+\Delta t}$). The marginal cost of charging and discharging is assumed to be zero.

$$\mathcal{U}_{y,s}^j = -f_y^Y \left[(3a) \right] \quad (3)$$

$$\sum_{n \in \mathcal{N}} \sum_{j \in \mathcal{S}_{j:n}} \delta I_{j:n, y}^j \cdot \Delta E_{j:n, y}^{j, \max} \quad (3a)$$

The existing network operator has hourly costs and benefits associated with existing generation (4a) and consumption (4b). Existing generators accrue hourly benefits through the sale of energy ($P_{\tilde{g}}^g$) on the spot market at a price (λ_n) higher than their marginal production cost ($C_{\tilde{g}}^g$). Consumers benefit when the price of energy λ_n is lower than the consumer's bid price (C_u^u) resulting in a surplus.

$$\mathcal{U}_{y,s}^e = f_y^H \sum_{t \in \mathcal{S}_t} \left[(4a) + (4b) \right] \quad (4)$$

$$\sum_{n \in \mathcal{N}^{\text{AC}}} \sum_{\tilde{g} \in \tilde{\mathcal{S}}_{g:n}} (-C_{\tilde{g}:n, t, y, s}^g) \cdot P_{\tilde{g}:n, t, y, s}^g \quad (4a)$$

$$\sum_{n \in \mathcal{N}^{\text{AC}}} \sum_{u \in \mathcal{S}_{u:n}} C_{u:n, t, y, s}^u \cdot P_{u:n, t, y, s}^u \quad (4b)$$

Combining (1)–(4) gives the global objective executed by an all knowing centralized authority to maximize the social welfare of the system (\mathcal{U}), as in (5). Social welfare is therefore defined as the sum over all scenarios \mathcal{S}_s of Gross Consumer Surplus (GCS) and net developer benefits. The final distribution of developer benefits and the GCS is calculated based on the resultant market clearing prices λ_n . The uncertainty of long term planning is captured by the probability π_s of occurrence of a given scenario. Multi-period planning is performed over the lifetime considering the years defined in set \mathcal{S}_y .

$$\max_{\mathcal{A}_w, \mathcal{A}_o, \mathcal{A}_j, \mathcal{A}_e} \mathcal{U} := \sum_{s \in \mathcal{S}_s} \pi_s \sum_{y \in \mathcal{S}_y} \mathcal{U}_{y,s}^w + \mathcal{U}_{y,s}^o + \mathcal{U}_{y,s}^j + \mathcal{U}_{y,s}^e \quad (5)$$

where

$$\begin{aligned} \mathcal{A}_w &= (\tilde{\mathbf{P}}^g, \Delta \tilde{\mathbf{P}}^{g, \max}), \quad \mathcal{A}_o = (\boldsymbol{\theta}, \boldsymbol{\alpha}^\ell, \Delta \mathbf{P}^{\zeta, \max}), \\ \mathcal{A}_j &= (\mathbf{P}^{j, \text{inj}}, \mathbf{P}^{j, \text{abs}}, \Delta \mathbf{E}^{j, \max}), \quad \mathcal{A}_e = (\tilde{\mathbf{P}}^g, \mathbf{P}^u) \end{aligned}$$

2) *Constraints*: Generation consisting of both RESs and conventional generation must remain within capacity limits. This is ensured by constraint (6). For RESs, parameter $\Psi_{\tilde{g}}^g$ is the per-unit RES generation time series and for conventional generators it is equal to one.

$$0 \leq P_{g:n, t, y, s}^g \leq \Psi_{\tilde{g}:n, t, y, s}^g \cdot P_{\tilde{g}:n, y}^{g, \max} \quad (6)$$

$$n \in \mathcal{N}^{\text{AC}}, \quad g \in \mathcal{S}_{g:n}, \quad t \in \mathcal{S}_t, \quad y \in \mathcal{S}_y, \quad s \in \mathcal{S}_s$$

In the particular case that the generator is a candidate OWPP under consideration for expansion, $P_{\tilde{g}}^{g, \max}$ is constrained from above by $\widehat{P}_{\tilde{g}}^{g, \max}$ and may only increase or remain constant year over year as in:

$$\begin{aligned} P_{\tilde{g}:n, y}^{g, \max} &\leq \widehat{P}_{\tilde{g}:n}^{g, \max}, \quad P_{\tilde{g}:n, y-\Delta y}^{g, \max} \leq P_{\tilde{g}:n, y}^{g, \max} \\ \tilde{g} &\in \tilde{\mathcal{S}}_{g:n}, \quad n \in \mathcal{N}^{\text{AC}}, \quad y \in \mathcal{S}_y, \end{aligned} \quad (7)$$

where Δy is the number of years between modelling years. $P_{\tilde{g}:n, y-\Delta y}^{g, \max}$ in the first year is assumed to be zero. Demand is set via time series Ψ_u^u as in (8). A high cost for load shedding ensures it is only a last resort.

$$0 \leq P_{u:n, t, y, s}^u \leq \Psi_{u:n, t, y, s}^u \quad (8)$$

$$n \in \mathcal{N}^{\text{AC}}, \quad u \in \mathcal{S}_{u:n}, \quad t \in \mathcal{S}_t, \quad y \in \mathcal{S}_y, \quad s \in \mathcal{S}_s$$

A storage device has a state of charge E_j^j at each time step Δt defined by the following constraint:

$$\begin{aligned} E_{j:n, t, y, s}^j &= (1 - \gamma_{j:n}^j)^{\Delta t} E_{j:n, t-\Delta t, y, s}^j \\ &+ \Delta t (\eta_{j:n}^{j, \text{abs}} P_{j:n, t, y, s}^{j, \text{abs}} - \frac{P_{j:n, t, y, s}^{j, \text{inj}}}{\eta_{j:n}^{j, \text{inj}}}) \end{aligned} \quad (9)$$

$$j \in \mathcal{S}_{j:n}, \quad n \in \mathcal{N}^{\text{AC}}, \quad t \in \mathcal{S}_t^*, \quad y \in \mathcal{S}_y, \quad s \in \mathcal{S}_s,$$

where \mathcal{S}_t^* denotes the set of all time steps except the first one. Here, γ_j^j is the self discharge rate and $\eta_j^{j, \text{abs}}$ and $\eta_j^{j, \text{inj}}$ are the charge and discharge efficiencies respectively.

The current state of charge is constrained between zero and the rating of the device $E_j^{j, \max}$. The device rating can be expanded up to a maximum of $\widehat{E}_j^{j, \max}$ but may only increase or remain constant year over year as in:

$$\left. \begin{aligned} 0 &\leq E_{j:n, t, y, s}^j \leq E_{j:n, y}^{j, \max} \\ E_{j:n, y-\Delta y}^{j, \max} &\leq E_{j:n, y}^{j, \max} \leq \widehat{E}_{j:n}^{j, \max} \end{aligned} \right\} \begin{aligned} n &\in \mathcal{N}^{\text{AC}}, \quad j \in \mathcal{S}_{j:n} \\ t &\in \mathcal{S}_t, \quad y \in \mathcal{S}_y \\ s &\in \mathcal{S}_s. \end{aligned} \quad (10)$$

In the first year, $E_{j:n, y-\Delta y}^j$ is assumed to be zero. A storage device has a maximum rate at which it can charge and discharge, this is ensured by (11). $\xi_j^{j, c}$ and $\xi_j^{j, d}$ are the normalized charge and discharge rates.

$$\left. \begin{aligned} 0 &\leq P_{j:n, t, y, s}^{j, \text{abs}} \leq \xi_{j:n}^{j, c} \cdot E_{j:n, y}^{j, \max} \\ 0 &\leq P_{j:n, t, y, s}^{j, \text{inj}} \leq \xi_{j:n}^{j, d} \cdot E_{j:n, y}^{j, \max} \end{aligned} \right\} \begin{aligned} n &\in \mathcal{N}^{\text{AC}}, \quad j \in \mathcal{S}_{j:n} \\ t &\in \mathcal{S}_t, \quad y \in \mathcal{S}_y \\ s &\in \mathcal{S}_s \end{aligned} \quad (11)$$

Constraint (12) sets the initial and final states of charge in each year to half capacity. The final constraint on storage, to not simultaneously charge and discharge is not explicitly en-

forced, rather, it is implicitly guaranteed via charge and discharge efficiencies less than one.

$$E_{j:n,1,y,s}^j = \frac{E_{j:n,y}^{j,\max}}{2} + \eta_{j:n}^{\text{j,abs}} P_{j:n,1,y,s}^{\text{j,abs}} - \frac{P_{j:n,1,y,s}^{\text{j,inj}}}{\eta_{j:n}^{\text{j,inj}}} \left. \begin{array}{l} n \in \mathcal{N}^{\text{AC}} \\ j \in \mathcal{S}_{j:n} \\ y \in \mathcal{S}_y \\ s \in \mathcal{S}_s \end{array} \right\} \quad (12)$$

$$E_{j:n,T,y,s}^j = \frac{E_{j:n,y}^{j,\max}}{2}$$

The AC and DC network constraints described below are implemented using the PowerModels(ACDC).jl packages [36], [37]. A bus injection model is used for AC network branches while considering the linear ‘‘DC’’ power flow approximations as in (13). Transformers are lumped into the branch model via the transformation ratio τ , which is unity when no transformer is required.

$$P_{l:mn,t,y,s}^\ell = \frac{b_{\bar{l}:\{mn\}}}{\tau} [\theta_{m,t,y,s} - \theta_{n,t,y,s}] \quad (13)$$

$$P_{l:mn,t,y,s}^\ell = \frac{b_{\bar{l}:\{mn\}}}{\tau} [\tilde{\theta}_{l:mn,t,y,s} - \tilde{\theta}_{l:nm,t,y,s}]$$

$$\begin{aligned} |P_{l:mn,t,y,s}^\ell| &\leq P_{l:\{mn\}}^{\ell,\max} \\ |P_{l:mn,t,y,s}^\ell| &\leq P_{l:\{mn\}}^{\ell,\max} \cdot \alpha_{l:\{mn\},y}^\ell \\ mn \in \mathcal{E}^{\text{AC}}, \quad \bar{l} \in \bar{\mathcal{S}}_{l:\{mn\}}^{\text{AC}}, \quad \tilde{l} \in \tilde{\mathcal{S}}_{l:\{mn\}}^{\text{AC}} \\ t \in \mathcal{S}_t, \quad y \in \mathcal{S}_y, \quad s \in \mathcal{S}_s \end{aligned} \quad (14)$$

Power flow through any branch must respect the branch limits as in (14). Nodal voltage angle limits and the maximum divergence between connected nodes are constrained by (15).

$$\begin{aligned} \theta^{\min} &\leq \theta_{n,t,y,s} \leq \theta^{\max} \\ |\theta_{n,t,y,s} - \theta_{m,t,y,s}| &\leq \Delta\theta^{\max} \\ \theta^{\min} &\leq \tilde{\theta}_{l:mn,t,y,s} \leq \theta^{\max} \\ |\tilde{\theta}_{l:mn,t,y,s} - \tilde{\theta}_{l:nm,t,y,s}| &\leq \Delta\theta^{\max} \\ |\tilde{\theta}_{l:mn,t,y,s} - \theta_{m,t,y,s}| &\leq (1 - \alpha_{l:\{mn\},y}^\ell) \cdot M \end{aligned} \left. \begin{array}{l} mn \in \mathcal{E}^{\text{AC}} \\ \tilde{l} \in \tilde{\mathcal{S}}_{l:\{mn\}}^{\text{AC}} \\ t \in \mathcal{S}_t \\ y \in \mathcal{S}_y \\ s \in \mathcal{S}_s \end{array} \right\} \quad (15)$$

The final constraint in (15) is only necessary when candidate branches are considered. This constraint leaves candidate line angles unconstrained when the branch is not included, i.e. $\alpha^\ell = 0$, while enforcing equality with the existing voltage angle when the branch is active, i.e. $\alpha^\ell = 1$. The AC network is linked to the DC network via an HVDC converter with a maximum AC side capacity of $P^{\zeta,\max}$. $P^{\zeta,\max}$ is constrained from above by $P^{\zeta,\max}$ and can only increase or remain constant year over year as in:

$$\begin{aligned} |P_{ne,t,y,s}^{\zeta,\text{AC}}| &\leq P_{ne,y}^{\zeta,\max} \\ P_{ne,y-\Delta y}^{\zeta,\max} &\leq P_{ne,y}^{\zeta,\max} \leq \widehat{P_{ne}^{\zeta,\max}} \end{aligned} \left. \begin{array}{l} ne \in \mathcal{E}^{\text{AC-DC}} \\ t \in \mathcal{S}_t \\ y \in \mathcal{S}_y \\ s \in \mathcal{S}_s \end{array} \right\} \quad (16)$$

The AC side power is linked to the DC side power through the non negative converter losses: L^ζ . This, and the upper limit on DC side power is set by:

$$\begin{aligned} |P_{en,t,y,s}^{\zeta,\text{DC}}| &\leq (L^\zeta - 1) P_{ne,y}^{\zeta,\max} \\ P_{ne,t,y,s}^{\zeta,\text{loss}} &= L^\zeta P_{ne,t,y,s}^{\zeta,\text{AC}} \geq 0 \\ P_{ne,t,y,s}^{\zeta,\text{AC}} + P_{en,t,y,s}^{\zeta,\text{DC}} &= P_{ne,t,y,s}^{\zeta,\text{loss}} \end{aligned} \left. \begin{array}{l} ne \in \mathcal{E}^{\text{AC-DC}} \\ t \in \mathcal{S}_t \\ y \in \mathcal{S}_y \\ s \in \mathcal{S}_s \end{array} \right\} \quad (17)$$

In the DC network, linearized power flow reduces to a network flow model (18). DC side power flow through transmission lines must remain within limits as in (19).

$$\begin{aligned} P_{l:ef,t,y,s}^\ell &= -P_{l:fe,t,y,s}^\ell \\ P_{l:ef,t,y,s}^\ell &= -P_{l:fe,t,y,s}^\ell \end{aligned} \quad (18)$$

$$\begin{aligned} |P_{l:ef,t,y,s}^\ell| &\leq P_{l:\{ef\}}^{\ell,\max} \\ |P_{l:ef,t,y,s}^\ell| &\leq P_{l:\{ef\}}^{\ell,\max} \cdot \alpha_{l:\{ef\},y}^\ell \\ ef \in \mathcal{E}^{\text{DC}}, \quad \bar{l} \in \bar{\mathcal{S}}_{l:\{ef\}}^{\text{DC}}, \quad \tilde{l} \in \tilde{\mathcal{S}}_{l:\{ef\}}^{\text{DC}} \\ t \in \mathcal{S}_t, \quad y \in \mathcal{S}_y, \quad s \in \mathcal{S}_s \end{aligned} \quad (19)$$

Finally, Kirchhoff’s current law must be satisfied for both AC and DC grids. On the AC side the nodal power balance is given by (20). The AC nodal balance equation is a complicating constraint that links the optimization variables. The dual variable of the constraint is λ_m , the marginal price of energy.

$$\begin{aligned} \sum_{e \in \mathcal{N}_m^{\text{DC}}} P_{me,t,y,s}^{\zeta,\text{AC}} - \sum_{n \in \mathcal{N}_m^{\text{AC}}} \sum_{l \in \mathcal{S}_{l:\{mn\}}^{\text{AC}}} P_{l:mn,t,y,s}^\ell \\ + \sum_{g \in \mathcal{S}_{g:n}} P_{g:m,t,y,s}^g - \sum_{u \in \mathcal{S}_{u:n}} P_{u:m,t,y,s}^u \\ + \sum_{j \in \mathcal{S}_{j:n}} P_{j:m,t,y,s}^{\text{j,inj}} - \sum_{j \in \mathcal{S}_{j:n}} P_{j:m,t,y,s}^{\text{j,abs}} = 0 \end{aligned} \left. \begin{array}{l} m \in \mathcal{N}^{\text{AC}} \\ t \in \mathcal{S}_t \\ y \in \mathcal{S}_y \\ s \in \mathcal{S}_s \\ (: \lambda_{m,t,y,s}) \end{array} \right\} \quad (20)$$

Here, $\mathcal{N}_m^{\text{AC}} := \{n \in \mathcal{N}^{\text{AC}} : mn \in \mathcal{E}^{\text{AC}}\}$ and $\mathcal{N}_m^{\text{DC}} := \{e \in \mathcal{N}^{\text{DC}} : me \in \mathcal{E}^{\text{AC-DC}}\}$ respectively denote the AC and DC neighbors of $m \in \mathcal{N}$. On the DC network side the nodal power balance equation is non complicating:

$$\sum_{m \in \mathcal{N}_e^{\text{AC}}} P_{em,t,y,s}^{\zeta,\text{DC}} + \sum_{f \in \mathcal{N}_e^{\text{DC}}} \sum_{l \in \mathcal{S}_{l:\{ef\}}^{\text{DC}}} P_{l:ef,t,y,s}^\ell = 0. \quad (21)$$

$$e \in \mathcal{N}^{\text{DC}}, \quad t \in \mathcal{S}_t, \quad y \in \mathcal{S}_y, \quad s \in \mathcal{S}_s.$$

B. Zonal Market Model

To model a zonal market we start by partitioning the network nodes into a set \mathcal{Z} of disjoint market zones, so that $\mathcal{N} = \bigcup_{z \in \mathcal{Z}} z$. The edges are also partitioned into inter-zonal edges $\mathcal{E}^{\text{te}} \subseteq \{mn : z \in \mathcal{Z}, m \in z, n \notin z\}$ and intra-zonal edges $\mathcal{E}^{\text{br}} \subseteq \{mn : z \in \mathcal{Z}, m \in z, n \in z\}$. For ease of notation, the optimization variables for transmission lines along these edges are denoted as $(\theta^{\text{te}}, \alpha^{\ell,\text{te}})$ and $(\theta^{\text{br}}, \alpha^{\ell,\text{br}})$, respectively. The superscripts refer to two new agents we will introduce, the Transmission Expansion agent (\mathcal{A}^{te}) and the Balancing Responsible agent (\mathcal{A}^{br}). We re-group the optimization variables into agents \mathcal{A}^{te} and \mathcal{A}^{br} as follows:

$$\mathcal{A}^{\text{te}} = (\mathcal{A}_w, \mathcal{A}_j, \mathcal{A}_e, \mathcal{A}_o^{\text{te}}) \quad \text{and} \quad \mathcal{A}^{\text{br}} = (\mathcal{A}_w, \mathcal{A}_j, \mathcal{A}_e, \mathcal{A}_o^{\text{br}}),$$

where $\mathcal{A}_o^{\text{te}}$ differs from \mathcal{A}_o in that the transmission lines considered are restricted to inter-zonal connections. $\mathcal{A}_o^{\text{br}}$ is the complement considering only intra-zonal connections. Further-

more, we define zonal power balance equations for both the AC and DC networks as in (22) and (23).

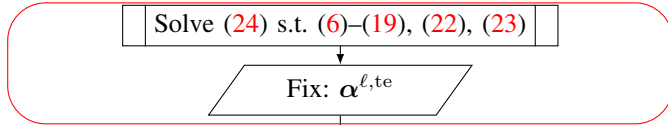
$$\left. \begin{aligned} & \sum_{m \in \mathcal{Z}} \left(\sum_{e \in \mathcal{N}_m^{\text{DC}}} P_{me,t,y,s}^{\zeta,\text{AC}} - \sum_{g \in \mathcal{S}_{g:n}} P_{g:m,t,y,s}^g \right) \\ & + \sum_{n \in \mathcal{N}_m^{\text{AC}}} \sum_{l \in \mathcal{S}_{\ell:\{mn\}}^{\text{te,AC}}} P_{l:mn,t,y,s}^\ell - \sum_{u \in \mathcal{S}_{u:n}} P_{u:m,t,y,s}^u \\ & + \sum_{j \in \mathcal{S}_{j:n}} P_{j:m,t,y,s}^{\text{j,inj}} - \sum_{j \in \mathcal{S}_{j:n}} P_{j:m,t,y,s}^{\text{j,abs}} \end{aligned} \right\} \begin{aligned} & z \in \mathcal{Z}, \\ & t \in \mathcal{S}_t, \\ & y \in \mathcal{S}_y, \\ & s \in \mathcal{S}_s, \\ & (: \lambda_{z,t,y,s}^z) \end{aligned} = 0 \quad (22)$$

$$\sum_{e \in \mathcal{Z}} \left(\sum_{m \in \mathcal{N}_e^{\text{AC}}} P_{em,t,y,s}^{\zeta,\text{DC}} + \sum_{f \in \mathcal{N}_e^{\text{DC}}} \sum_{l \in \mathcal{S}_{\ell:\{ef\}}^{\text{te,DC}}} P_{l:ef,t,y,s}^\ell \right) = 0 \quad (23)$$

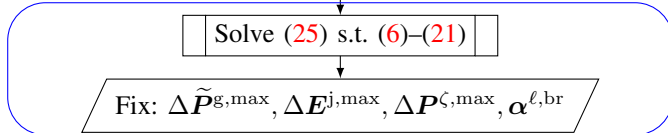
$$z \in \mathcal{Z}, \quad t \in \mathcal{S}_t, \quad y \in \mathcal{S}_y, \quad s \in \mathcal{S}_s$$

In a zonal market, (22) provides the market clearing condition. The dual variable of the constraint is the marginal price of energy at all nodes within zone z . As all nodes in a single market zone have a common energy price, the price signals of congestion are suppressed. This further complicates the already difficult problem of GATE. To overcome this difficulty a multi-level approach is adopted, whereby expansion planning is achieved via a four step solution method. This solution method is presented in fig. 2.

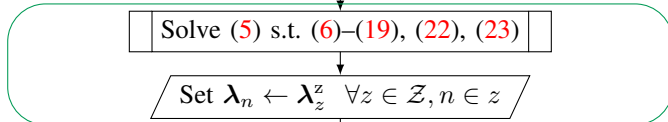
Find Inter-Zonal Network



Find Intra-Zonal Network



Forecast Power Flows



Correct Nodal Imbalance

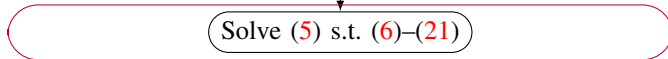


Figure 2: Flowchart of solution method for zonal market clearing formulation. “Solve” refers to the specified equations considering the fixed decision variables found previously.

Step one is to calculate the inter-zonal network expansion. Agent \mathcal{A}^{te} solves (24) ((5) with (24a) substituted for (2a)) subject to constraints (6) through (19) and the zonal power balance constraints (22) and (23). This determines the location and capacity of transmission lines between market zones. The variables $\alpha^{\ell,\text{te}}$ are passed to agent \mathcal{A}^{br} to perform intra-zonal transmission and generation expansion.

$$\begin{aligned} \max_{\mathcal{A}^{\text{te}}} \mathcal{U} := & \sum_{s \in \mathcal{S}_s} \pi_s \sum_{y \in \mathcal{S}_y} f_y^{\text{H}} \sum_{t \in \mathcal{S}_t} \left[(4\text{a}) + (4\text{b}) \right] \\ & - f_y^{\text{Y}} \left[(1\text{a}) + (2\text{b}) + (3\text{a}) + (24\text{a}) \right] \\ & \sum_{\substack{\{mn\} \subseteq \mathcal{N} \\ mn \in \mathcal{E}^{\text{te}}}} \sum_{l \in \tilde{\mathcal{S}}_{\ell:\{mn\}}} \alpha_{l:\{mn\},y}^{\ell,\text{te}} \cdot \tilde{I}_{l,y} \end{aligned} \quad (24)$$

Step two is to calculate intra-zonal expansion. This is performed by agent \mathcal{A}^{br} while respecting the inter-zonal capacity limitations as well as nodal power balance. Hence, objective (25) ((5) with (25a) substituted for (2a)) is solved subject to nodal power balance (20) and (21) as well as the remaining network constraints (6) through (19). To achieve nodal balance at the lowest cost, agent \mathcal{A}^{br} has the option to eliminate intra-zonal congestion via the construction of new lines $\alpha^{\ell,\text{br}}$, the expansion or reduction of newly added OWPPs and/or storage $(\tilde{P}_g^{\text{g,max}}, E_j^{\text{j,max}})$ or the curtailment and/or re-dispatch of network generators (S_g) .

$$\begin{aligned} \max_{\mathcal{A}^{\text{br}}} \mathcal{U} := & \sum_{s \in \mathcal{S}_s} \pi_s \sum_{y \in \mathcal{S}_y} f_y^{\text{H}} \sum_{t \in \mathcal{S}_t} \left[(4\text{a}) + (4\text{b}) \right] \\ & - f_y^{\text{Y}} \left[(1\text{a}) + (2\text{b}) + (3\text{a}) + (25\text{a}) \right] \\ & \sum_{\substack{\{mn\} \subseteq \mathcal{N} \\ mn \in \mathcal{E}^{\text{br}}}} \sum_{l \in \tilde{\mathcal{S}}_{\ell:\{mn\}}} \alpha_{l:\{mn\},y}^{\ell,\text{br}} \cdot \tilde{I}_{l:\{mn\},y} \end{aligned} \quad (25)$$

Step three is performed post network expansion. A power auction is held considering only inter-zonal capacity constraints. This step simulates the day ahead spot market and provides the forecast of inter zonal power flows and the zonal market clearing prices based on an optimal dispatch. In the case of congestion free power flows this is the final step. When congestion is present, the additional step of re-dispatch is needed to relieve congestion and balance the network.

Step four: re-dispatch. The final cost of a zonally cleared energy market depends on the re-dispatching mechanism chosen. In the EU both market and regulatory based re-dispatch exists [40]. In this work we have chosen an idealized RDCC and argue that this represents an upper bound on possible zonal market benefits. Our argument is as follows.

In RDCC, an all knowing balancing authority calls on the lowest cost available generation and/or load to up or down regulate during re-balancing actions. Generators required to up regulate are compensated at their marginal price, while those required to down regulate are permitted to keep profits made from the spot market but must return any avoided variable costs (e.g. unused fuel costs). Since participants in RDCC are contractually obliged to participate at their marginal rates and we are assuming perfect transparency from generators regarding their marginal cost and available capacity, a market based re-dispatch could only, at best, achieve an identical re-dispatch cost.

Of course, in practice, the assumption of perfect transparency by market participants is unrealistic as this requires the sharing of private information. As such, we are not arguing RDCC is better than a market based re-dispatch mechanism.

Rather, that in its idealized form it describes the upper bound on efficient re-dispatch.

Together, steps one through four describe the approach used for GATE planning in zonal markets. Alone, steps three and four describe an energy auction which can be run on any topology previously determined. For example, a topology determined using the nodal market approach described in section III-A can be operated within a zonal market structure.

IV. TEST CASE

A. Domain

A test grid (\mathcal{G}) in the North Sea is modelled. The onshore and offshore nodes considered are displayed in fig. 3 and their coordinates listed in table IX of the appendix.

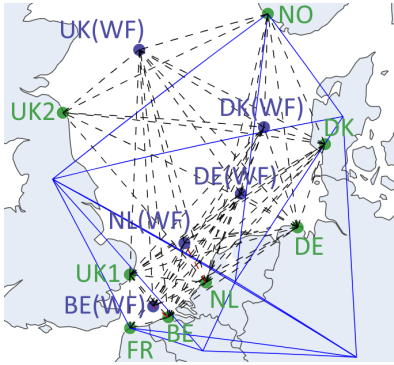


Figure 3: North Sea domain. Lines: NTCs (solid blue), HVDC (dashed black), HVAC (dashed red).

Table I: Infrastructure costs (excluding cables).

Component	OWPPs	Onshore converters	Offshore converters	Onshore storage	Offshore storage
Cost	2100	192.5	577.5	183	275

*Costs are in €/kW and €/kWh (storage)

B. Candidate Expansion

Candidate generation, transmission and storage assets can be expanded at a cost specified in table I. The maximum allowable capacity for OWPPs ($P_{g,\max}^{\widehat{}}$), HVDC converters ($P_{c,\max}^{\widehat{}}$) and storage ($E_{s,\max}^{\widehat{}}$) are listed in table IX of the appendix. At onshore nodes a dimensioning incident of 3 GW is assumed, hence onshore converters are limited to 3 GW while offshore converters can reach sizes of 4 GW. Storage is assumed to be a four hour duration, lithium ion system. Candidate connections for HVAC and HVDC are shown in fig. 3. The details of the candidate cables included in each connection as well as their costs are summarized in tables V and VI of the appendix.

C. Existing Generation

The existing energy mix (\bar{P}^g) in each country is sourced from the ENTSO-E TYNDP, which provides a baseline as well as futures scenarios for the energy mix of European countries. The projected scenarios are for years 2030 and 2040 [41], [5]. Further details are provided below. Assumptions for marginal costs of generating sources are listed in table VII of the appendix.

D. Onshore grid

The Net Transfer Capacities (NTCs) between the selected countries as provided in the TYNDP are modeled as existing transmission lines. They are displayed in fig. 3 and listed in table VIII of the Appendix. The onshore NTCs remain static through the simulation years.

E. Demand

Hourly demand data (P^u) is taken from the TYNDP. Meeting demand at all times is ideal. When this is not possible, however, load defined as Demand Side Response (DSR) can be shed at a cost 119 €/MWh. In the event that further load must be shed, the Value Of Lost Load (VOLL) is 5 k€/MWh. DSR does affect market price formation while load shedding does not. During times of extreme energy scarcity such as load shedding events an energy price cap of 180 €/MWh is enforced based on EU regulation 2022/1854 [42]. GCS is calculated based on a constant consumer bid price of 150 €/MWh.

F. Scenarios

In the TYNDP, projections are made for future generation and demand via scenarios that consider different paths towards a net zero 2050. In this study the National Trends (NT), Distributed Generation (DG) and Global Ambition (GA) scenarios are included. In brief, NT is based on the National Energy Climate Policies, DG assumes mass societal adoption of distributed RES and GA considers a global movement towards the targets of the Paris Agreement. For further details we refer the reader to the TYNDP [5]. Pairing historical RES generation time series (Ψ^g) from years 2014 and 2015 results in six scenarios in \mathcal{S}_s . Each are considered to have an equally likely probability of occurrence π_s .

Due to computational requirements each simulation year is clustered into four 24-hour days. The simulation years are 2020, 2030 and 2040. The representative days are found via the k -medoids clustering method [43]. The temporal correlation between the various time series is maintained. Ten calendar years per simulation year are considered: 2020-2029 is modelled with 2020 data, 2030-2039 with 2030 data and 2040-2049 with 2040 data.

V. RESULTS

The presented methodology is applied to \mathcal{G} to compare the effects of an nOBZ, zOBZ and an HMD considering multiple OWPPs. The market structure case studies are as follows:

- Each OWPP is part of its home market zone (HMD).
- All OWPPs form a common offshore market (zOBZ).
- Each node is its own market zone (nOBZ).

The resulting topologies are displayed in fig. 4 through 6. The figures present the selected transmission lines and their capacities as well as the build schedule. The same information is provided for the OWPPs, HVDC converters and storage in table II. In all topologies, HOAs are dominant features. Only in the HMD and only for the closest wind development region to shore (Belgium) is a radial connection selected.

A breakdown of transmission, OWPP and storage developer costs and benefits are provided in table III. The net benefits,

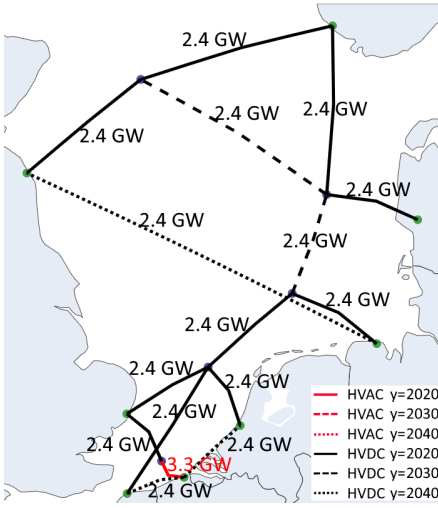
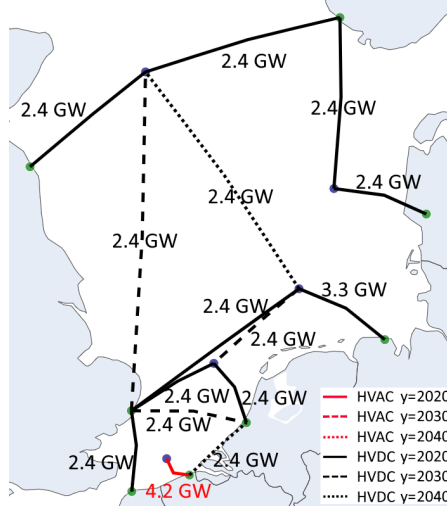
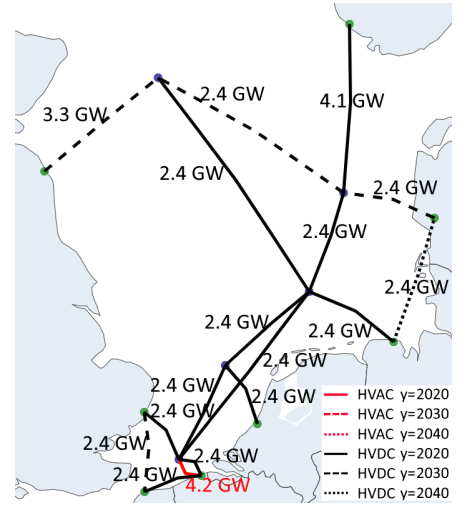
Figure 4: nOBZ \mathcal{G} topology.Figure 5: HMD \mathcal{G} topology.Figure 6: zOBZ \mathcal{G} topology.

TABLE II
EXPANSION PLANNING SCHEDULE OF GRID \mathcal{G} .

Year	nOBZ			HMD			zOBZ		
	'20	'30	'40	'20	'30	'40	'20	'30	'40
	$P_{ne,y}^{C,\max}$ [GW]								
UK1	2.9	3	3	3	3	3	2.4	3	3
FR	2.4	2.4	3	2.4	2.4	2.4	2.4	3	3
BE	0	0	1.8	0	0	2.4	0	0.6	1.5
NL	2.4	2.4	3	2.4	3	3	2.4	2.4	2.4
DE	2.4	2.4	3	3	3	3	2.4	2.4	3
DK	1.6	2.4	2.4	1.7	1.9	1.9	0	2.4	2.4
NO	3	3	3	3	3	3	3	3	3
UK2	1.9	2.4	3	1.7	2.4	2.4	0	3	3
BE(WF)	0.5	0.6	0.6	0	0	0	0	0	0
DE(WF)	3.7	3.7	3.7	3.7	3.7	3.7	3.6	3.7	3.7
NL(WF)	3.8	3.8	3.8	3.8	3.8	3.8	3.8	3.8	3.8
DK(WF)	3.7	3.7	3.8	3.7	3.7	3.8	3.7	3.7	3.8
UK(WF)	3.2	3.4	3.6	3.2	3.4	3.6	2.4	3.4	3.6

OWPPs: All 4 GW in 2020 (nOBZ, HMD).
All 4 GW in 2020 except UK(WF) is 3.9 GW in 2020, then expanded to 4 GW in 2030 (zOBZ).
Storage: 1 GWh of storage is scheduled in Holland in 2040 (nOBZ, HMD, zOBZ).

TABLE III
SUMMARY OF COSTS AND BENEFITS FOR \mathcal{G} IN B€.

	Transmission		OWPP		Storage	
	Cost	Benefits	Cost	Benefits	Cost	Benefits
nOBZ	21.754	64.147	42.000	134.135	0.059	0.058
HMD*	22.380	64.722	42.000	133.700	0.059	0.058
zOBZ*	22.984	70.453	41.885	125.568	0.059	0.057
zOBZ	22.984	57.703	41.885	135.241	0.059	0.056
nOBZ**	21.754	53.452	42.000	139.866	0.059	0.057
nOBZ*	21.754	49.015	42.000	143.459	0.059	0.047
HMD	22.380	48.526	42.000	144.152	0.059	0.046

HMD*: The HMD topology operating in an nOBZ market.
zOBZ*: The zOBZ topology operating in an nOBZ market.
nOBZ*: The nOBZ topology operating in an HMD market.
nOBZ**: The nOBZ topology operating in a zOBZ market.

GCS and re-dispatch costs of each topology are ranked by social welfare in table IV.

There is little difference between the social welfare obtained under all variations of the nodal market structure (nOBZ, HMD* and zOBZ*). Three different topologies, all with similar levels of social welfare and a global lower bound (nOBZ), effectively demonstrate the flatness of the solution space and

TABLE IV
SUMMARY OF SOCIAL WELFARE FOR \mathcal{G} IN B€.

	Net Benefit	GCS	Re-dispatch	Social Welfare	Difference [%]
nOBZ	134.527	1920.331	0.000	2054.858	-
HMD*	134.040	1920.299	0.000	2054.340	-0.03
zOBZ*	131.151	1922.617	0.000	2053.767	-0.05
zOBZ	128.073	1926.606	128.596	1926.083	-6.27
nOBZ**	129.561	1921.987	127.006	1924.543	-6.34
nOBZ*	128.707	1924.729	145.615	1907.821	-7.16
HMD	128.284	1916.556	155.168	1889.672	-8.04

*-entries in the first column are as in table III.

The last column is the change in social welfare compared to the nOBZ.

hence the limited value attached to the certificate of optimality. Planners should therefore not be overly concerned about developing a uniquely optimal configuration as the problem's uncertainty dwarfs the difference between a good solution and the best solution.

The benefit of using a nodal based pricing mechanism is clearly demonstrated. All zonal pricing models result in a decrease in social welfare of 6-8% compared to nodal pricing. The worst performing market structure is the HMD. It seems, knowing the market structure a priori is not essential from a planning perspective as each design operates relatively well under a changing market design.

Despite the poor performance of the zonal market models in the zonal markets for which they were intended, the high quality of their nodal market variations suggest merit from a decomposition perspective. The computation times for the approaches are: zOBZ/HMD: ≈ 2.5 hours, the nOBZ: halted after twelve hours with a small optimality gap of 0.04% remaining. Zonal models scale better than nodal due to the natural decomposition along intra and inter zonal lines.

The three nodal market models may have little variation in social welfare but do have variation in how agent benefits are distributed. For example, nOBZ results in 6.8% higher benefits for an OWPP developer than in zOBZ*. There is no free lunch of course as this is at the expense of the transmission developer which sees a decrease in benefits of 9%. The ability to adjust the distribution of benefits among stakeholders

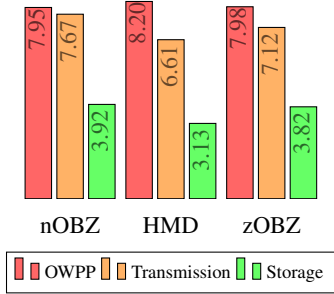


Figure 7: Yearly percent return on investment for \mathcal{G} .

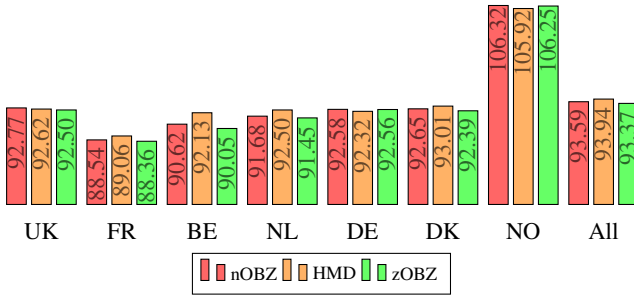


Figure 8: Average onshore energy prices for \mathcal{G} [€/MWh].

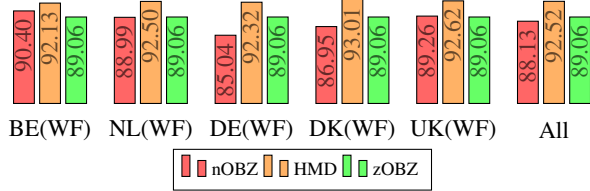


Figure 9: Average offshore energy prices for \mathcal{G} [€/MWh].

without sacrificing overall social welfare may prove useful.

All market mechanisms result in a positive return on investment for all agents (fig. 7). The highest return for transmission and storage developers occurs under an nOBZ while OWPP developers do best in an HMD. By examining the average energy prices per node in figs. 8 and 9 we see why. The HMD has the highest average energy prices both offshore and onshore. While this translates to higher profits for OWPP developers, it is bad for consumers and lowers the overall social welfare. The average European wide energy price for the HMD is 93.23 €/MWh, for the zOBZ it is 91.21 €/MWh and for the nOBZ it is 90.86 €/MWh.

There is very little difference in wind curtailment between market designs, which amounts to essentially zero. This is shown in fig. 10. Although the zOBZ results in about three times the curtailment compared to the nOBZ and the HMD, it is still only about 0.5% of the total energy production.

The cost to re-dispatch varies substantially between zonal market models. The highest re-dispatch costs are associated with Home market designs and the lowest with zonal OBZs. A breakdown of the re-dispatch costs by generation type is presented in fig. 11. It is interesting that in the home market designs load shedding makes up about 5% of the overall re-dispatch cost. It is not that more load is shed in this

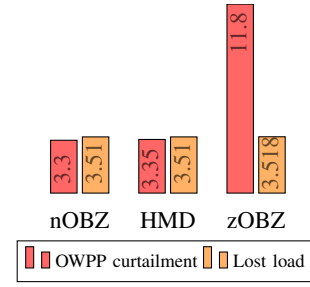


Figure 10: OWPP curtailment and lost load in TWh. Potential OWPP production: 2287 TWh (nOBZ/HMD), 2284 TWh (zOBZ). Total load: 50366 TWh.

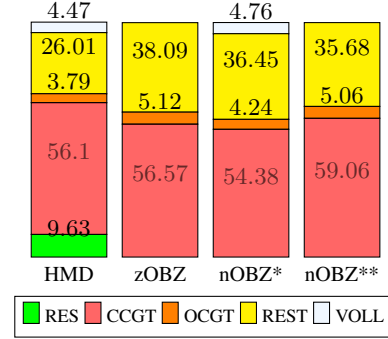


Figure 11: Percent breakdown of re-dispatch costs.

market structure, as load shedding is fairly constant at about 3.5 TWh across all market models (fig. 10), but rather that the onshore-offshore congestion constraint is binding but not enforced. This is a variation on the pivotal supplier problem discussed in section II with the exception that VOLL does not affect the spot price formulation so the zOBZ and nOBZ** see the energy price cap of 180 €/MWh rather than the 5k€/MWh for VOLL avoiding windfall profits for generators.

It is worth discussing the low level of storage selected in all topologies. This may be due to too high a cost or is possibly a modelling deficiency as type specific generation constraints are not implemented. Ramping times, start up costs and seasonality are completely ignored. To fully capture the benefits of storage some further level of detail may be necessary. For example, Norway has over 24 GW of pumped storage that is highly seasonal. Modelling this seasonality constraint (among others) might be necessary to effectively access the value of additional storage assets. This investigation is saved for future work.

VI. CONCLUSION

In this work, a generation and transmission expansion planning model for nodal and zonal market designs is developed, with the objective of maximizing a social welfare function consisting of net benefits for the generation, storage and transmission system developers and GCS. The developed model is applied to a test case in the North Sea (\mathcal{G}) to investigate the impact of market design on the optimal network topology.

From our study of \mathcal{G} we draw the following conclusions. HOAs are an important and cost effective feature of offshore transmission topologies. The nodal pricing structure results in the highest social welfare. The solution space around the optimal nodal market solution is quite flat and multiple solutions

of acceptable quality exist. A zonal planning approach has computational advantages over a nodal one and may be an effective decomposition strategy for larger problems. A topology developed assuming one market structure can operate well under a different market structure. The lowest European wide average energy price occurs in the nOBZ and the highest in the HMD. The pivotal supplier effect is present in re-dispatch of zonal markets as demonstrated in the HMD.

From the conducted analysis we conclude that generation and transmission planning should be carried out under the assumption that a nodal offshore bidding zone will be implemented as the obtained topology also performs well under changing market designs. When computational power becomes a constraint, however, a decomposition strategy based on a zonal market design may be used. More efficient and structure-exploiting optimization strategies, based e.g. on fast consensus ADMM [44] or Bender's decomposition [22], are also considered for future extensions.

REFERENCES

- [1] European Commission, "Re power EU with clean energy," 2022.
- [2] D. Jorgensen, T. Van der Straeten, R. Jetten, and R. Habeck, "The declaration of energy ministers on the North Sea as a green power plant of Europe," 2022.
- [3] "The Paris Agreement," united Nations Treaty Collection XXVII 7.d.
- [4] R. O'Sullivan, "Offshore wind in Europe key trends and statistics 2020," Wind Europe, Tech. Rep., 2021.
- [5] "ENTSOE TYNDP Ten year network development plan," accessed: 2022-05-17. [Online]. Available: <https://2022.entsoe-tyndp-scenarios.eu/>
- [6] European Commission, "Regulation (eu) 2022/869 of the european parliament and of the council of 30 may 2022," *Official Journal of the European Union*, 2022.
- [7] D. Van Hertem and M. Ghandhari, "Multi-terminal VSC HVDC for the European supergrid: Obstacles," *Renewable and sustainable energy reviews*, vol. 14, no. 9, pp. 3156–3163, 2010.
- [8] J. De Decker and A. Woyte, "Review of the various proposals for the European offshore grid," *Renewable energy*, vol. 49, pp. 58–62, 2013.
- [9] T. K. Vrana and O. B. Fosso, "Technical aspects of the North Sea super grid," *CIGRE Electra*, nov 2011.
- [10] J.-B. Curis, J. Descloux, N. Grisey *et al.*, "Deliverable 1.3: Synthesis of available studies on offshore meshed HVDC grids," 2016.
- [11] E. Pierri, O. Binder, N. G. Hemdan, and M. Kurrat, "Challenges and opportunities for a European HVDC grid," *Renewable and Sustainable Energy Reviews*, vol. 70, pp. 427–456, 2017.
- [12] A. J. Conejo, L. Baringo, S. J. Kazempour, and A. S. Siddiqui, *Generation and Transmission Expansion Planning*. Cham: Springer International Publishing, 2016, pp. 115–167.
- [13] B. Stott, J. Jardim, and O. Alsac, "DC power flow revisited," *IEEE transactions on power systems*, vol. 24, no. 3, pp. 1290–1300, 2009.
- [14] J. A. Taylor and F. S. Hover, "Convex models of distribution system reconfiguration," *IEEE Transactions on Power Systems*, vol. 27, no. 3, pp. 1407–1413, 2012.
- [15] H. Ergun, J. Dave, D. Van Hertem, and F. Geth, "Optimal power flow for ACDC grids: Formulation, convex relaxation, linear approximation, and implementation," *IEEE Transactions on Power Systems*, vol. 34, no. 4, pp. 2980–2990, jul 2019.
- [16] J. Dave, H. Ergun, and D. Van Hertem, "Relaxations and approximations of HVDC grid TNEP problem," *Electric power systems research*, vol. 192, p. 106683, 2021.
- [17] L. Baringo and A. J. Conejo, "Transmission and wind power investment," *IEEE transactions on power systems*, vol. 27, no. 2, pp. 885–893, 2012.
- [18] Y. Zhou, L. Wang, and J. D. McCalley, "Designing effective and efficient incentive policies for renewable energy in generation expansion planning," *Applied Energy*, vol. 88, no. 6, pp. 2201–2209, 2011.
- [19] A. Chuang, F. Wu, and P. Varaiya, "A game-theoretic model for generation expansion planning: problem formulation and numerical comparisons," *IEEE Transactions on Power Systems*, vol. 16, no. 4, pp. 885–891, 2001.
- [20] F. H. Murphy and Y. Smeers, "Generation capacity expansion in imperfectly competitive restructured electricity markets," *Operations research*, vol. 53, no. 4, pp. 646–661, 2005.
- [21] J. Wang, M. Shahidehpour, Z. Li, and A. Botterud, "Strategic generation capacity expansion planning with incomplete information," *IEEE Transactions on Power Systems*, vol. 24, no. 2, pp. 1002–1010, 2009.
- [22] L. Baringo and A. J. Conejo, "Wind power investment: A benders decomposition approach," *IEEE Transactions on Power Systems*, vol. 27, no. 1, pp. 433–441, 2012.
- [23] A. Botterud, M. Ilic, and I. Wangensteen, "Optimal investments in power generation under centralized and decentralized decision making," *IEEE Transactions on Power Systems*, vol. 20, no. 1, pp. 254–263, 2005.
- [24] J. Lopez, K. Ponnambalam, and V. Quintana, "Generation and transmission expansion under risk using stochastic programming," *IEEE transactions on power systems*, vol. 22, no. 3, pp. 1369–1378, 2007.
- [25] S. J. Kazempour, A. J. Conejo, and C. Ruiz, "Strategic generation investment using a complementarity approach," *IEEE Transactions on Power Systems*, vol. 26, no. 2, pp. 940–948, 2011.
- [26] S. J. Kazempour and A. J. Conejo, "Strategic generation investment under uncertainty via benders decomposition," *IEEE Transactions on Power Systems*, vol. 27, no. 1, pp. 424–432, 2012.
- [27] X. Zhang and A. J. Conejo, "Robust transmission expansion planning representing long- and short-term uncertainty," *IEEE Transactions on Power Systems*, vol. 33, no. 2, pp. 1329–1338, 2018.
- [28] R. A. Jabr, "Robust transmission network expansion planning with uncertain renewable generation and loads," *IEEE Transactions on Power Systems*, vol. 28, no. 4, pp. 4558–4567, 2013.
- [29] B. Chen, J. Wang, L. Wang, Y. He, and Z. Wang, "Robust optimization for transmission expansion planning: Minimax cost vs. minimax regret," *IEEE Transactions on Power Systems*, vol. 29, no. 6, pp. 3069–3077, 2014.
- [30] V. Grimm, A. Martin, M. Schmidt, M. Weibelzahl, and G. Zöttl, "Transmission and generation investment in electricity markets: The effects of market splitting and network fee regimes," *European journal of operational research*, vol. 254, no. 2, pp. 493–509, 2016.
- [31] L. P. Garces, A. J. Conejo, R. Garcia-Bertrand, and R. Romero, "A bilevel approach to transmission expansion planning within a market environment," *IEEE Transactions on Power Systems*, vol. 24, no. 3, pp. 1513–1522, 2009.
- [32] "ENTSO-E position on offshore development market and regulatory issues," 2020.
- [33] D. Schönheit, M. Kenis, L. Lorenz, D. Möst, E. Delarue, and K. Bruninx, "Toward a fundamental understanding of flow-based market coupling for cross-border electricity trading," *Advances in Applied Energy*, vol. 2, p. 100027, 2021.
- [34] *Market arrangements for offshore hybrid projects in the North Sea*, 2020.
- [35] H. Ergun, I. B. Sperstad, B. Espen Flo *et al.*, "Probabilistic optimization of t&d systems planning with high grid flexibility and its scalability," KU Leuven, Tech. Rep., 2021.
- [36] J. Bezanson, A. Edelman, S. Karpinski, and V. B. Shah, "Julia: A fresh approach to numerical computing," *SIAM review*, vol. 59, no. 1, pp. 65–98, 2017.
- [37] J. Dave, H. Ergun, T. An, J. Lu, and D. Van Hertem, "TNEP of meshed HVDC grids: 'AC', DC and convex formulations," *IET Generation, Transmission and Distribution*, vol. 13, pp. 5523–5532(9), dec 2019.
- [38] L. Gurobi Optimization, "Gurobi optimizer reference manual," 2020. [Online]. Available: <http://www.gurobi.com>
- [39] A. Moser, N. Bracht, and A. Maaz, "Simulating electricity market bidding and price caps in the European power markets s18 report," European Commission and Directorate-General for Energy, Tech. Rep., 2017.
- [40] L. Hirth and I. Schlecht, "Market-based redispatch in zonal electricity markets," *IO: Empirical Studies of Firms & Markets eJournal*, 2018.
- [41] ENTSO-E, "Data set: Tyndp 2020 scenario file."
- [42] European Commission, "Council regulation EU 2022/1854 of 6 October 2022 on an emergency intervention to address high energy prices," *Official Journal of the European Union*, 2022.
- [43] L. Kaufman and P. Rousseeuw, *Partitioning Around Medoids (Program PAM)*. John Wiley & Sons, Ltd, 1990, pp. 68–125.
- [44] A. Themelis, L. Stella, and P. Patrinos, "Douglas-Rachford splitting and ADMM for nonconvex optimization: Accelerated and Newton-type algorithms," *Computational Optimization and Applications*, vol. 82, pp. 395–440, 2022.
- [45] PROMOTiON Workpackage 1, "Cost data collection report," KU Leuven, Tech. Rep., 2020, (Internal document).
- [46] ABB high voltage cable unit, "HVDC light cables, submarine and land power cables," ABB, Tech. Rep., 2006.

VII. APPENDIX

TABLE V

HVAC AND HVDC CANDIDATE TRANSMISSION LINES

Routes			Candidate Cables (S_ℓ)
start	end	km	\mathcal{G}
UK1	FR	175	DC1-DC3
UK1	BE	188	DC1-DC3
UK1	NL	250	DC1-DC3
UK1	DE	565	DC1-DC3
UK1	DK	754	DC1-DC3
UK1	BE(WF)	129	DC1-DC3
UK1	DE(WF)	443	DC1-DC3
UK1	NL(WF)	204	DC1-DC3
UK1	DK(WF)	639	DC1-DC3
UK1	UK(WF)	716	DC1-DC3
FR	BE	130	DC1-DC3
FR	DE(WF)	565	DC1-DC3
FR	NL(WF)	328	DC1-DC3
BE	NL	168	DC1-DC3
BE	DE	511	DC1-DC3
BE	DK	752	DC1-DC3
BE	BE(WF)	61	DC1-DC3, AC1-AC3
BE	DE(WF)	464	DC1-DC3
BE	NL(WF)	247	DC1-DC3
BE	DK(WF)	684	DC1-DC3
BE	UK(WF)	859	DC1-DC3
NL	DE	346	DC1-DC3
NL	DK	586	DC1-DC3
NL	NO	873	DC1-DC3
NL	UK2	713	DC1-DC3
NL	BE(WF)	189	DC1-DC3
NL	DE(WF)	308	DC1-DC3
NL	NL(WF)	146	DC1-DC3, AC4, AC5
NL	DK(WF)	531	DC1-DC3
NL	UK(WF)	770	DC1-DC3
DE	DK	280	DC1-DC3
DE	NO	679	DC1-DC3
DE	UK2	834	DC1-DC3
DE	BE(WF)	534	DC1-DC3
DE	DE(WF)	212	DC1-DC3
DE	NL(WF)	369	DC1-DC3
DE	DK(WF)	337	DC1-DC3
DE	UK(WF)	753	DC1-DC3
DK	NO	444	DC1-DC3
DK	UK2	836	DC1-DC3
DK	BE(WF)	761	DC1-DC3
DK	DE(WF)	311	DC1-DC3
DK	NL(WF)	550	DC1-DC3
DK	DK(WF)	201	DC1-DC3
DK	UK(WF)	654	DC1-DC3
NO	UK2	711	DC1-DC3
NO	DE(WF)	571	DC1-DC3
NO	DK(WF)	353	DC1-DC3
NO	UK(WF)	414	DC1-DC3
UK2	DK(WF)	638	DC1-DC3
UK2	UK(WF)	311	DC1-DC3
BE(WF)	DE(WF)	462	DC1-DC3
BE(WF)	NL(WF)	229	DC1-DC3
BE(WF)	DK(WF)	677	DC1-DC3
BE(WF)	UK(WF)	820	DC1-DC3
DE(WF)	NL(WF)	241	DC1-DC3
DE(WF)	DK(WF)	223	DC1-DC3
DE(WF)	UK(WF)	556	DC1-DC3
NL(WF)	DK(WF)	449	DC1-DC3
NL(WF)	UK(WF)	630	DC1-DC3
DK(WF)	UK(WF)	460	DC1-DC3

Note: The specified lengths are 125% of the Euclidean distances to account for obstructions in the shortest path.

Table VI: HVAC(DC) candidate cables [45], [46].

	n-cm ²	MVA	km	Cost
AC1	12.16	4213	61	1520 M€
AC2	11.10	3319	61	1065 M€
AC3	8.10	2414	61	785 M€
AC4	11.16	3236	146	3345 M€
AC5	12.6.3	2479	146	2338 M€
DC1	4.15	4085	-	3.593 M€/km
DC2	4.10	3288	-	3.194 M€/km
DC3	2.20	2407	-	2.575 M€/km

*Specific HVAC cables are listed since capacity is dependent on length due to reactive power.

Table VII: Marginal price of generators [41].

Generation Type	€/MWh
PV, Hydro	18
Onshore wind	25
Offshore wind	59
Other RES	60
Gas CCGT	89
Nuclear	110
DSR	119
Gas OCGT, Coal, Pump storage, P2G,	120
Other non-RES	
Light oil	140
Heavy oil, Shale oil	150

UK-FR	UK-BE	UK-NL	UK-DE	UK-DK
4	1	1	1.4	1.4
UK-NO	FR-BE	FR-DE	BE-NL	BE-DE
2.8	4.3	3	2.4	1
NL-DE	NL-DK	NL-NO	DE-DK	DK-NO
5	0.7	0.7	3.5	1.64

Table VIII: Net transfer capacities between countries in GW [41].

TABLE IX
LOCATION OF NODES IN TEST GRIDS AND MAXIMUM CAPACITY OF CANDIDATE INFRASTRUCTURE.

Point	Longitude	Latitude	$P\zeta, \max$ [GW]	Pg, \max [GW]	Ej, \max [GWh]
UK1	52.21025	1.57374	3.0	-	1.0
FR	50.96332	1.82967	3.0	-	1.0
BE	51.32081	3.20768	3.0	-	1.0
NL	52.22215	4.49556	3.0	-	1.0
DE	53.67043	7.84620	3.0	-	1.0
DK	55.61420	8.72899	3.0	-	1.0
NO	58.43791	6.00292	3.0	-	1.0
UK2	55.68940	-1.91052	3.0	-	1.0
BE(WF)	51.53509	2.59644	4.0	4.0	0.02
NL(WF)	53.08300	3.51802	4.0	4.0	0.02
DE(WF)	54.34610	5.52400	4.0	4.0	0.02
DK(WF)	55.90115	6.22240	4.0	4.0	0.02
UK(WF)	57.33721	0.81425	4.0	4.0	0.02